Design of a thermoforming machine for the manufacture of ABS and PLA filament

Diseño de una máquina de termoconformados para la fabricación de filamento ABS Y PLA

Ricardo Andrés García-León[1]
Breiner Argotta-Hernandez[2]
Wilder Quintero-Quintero[3]

[1]Universidad Francisco de Paula Santander Ocaña (Colombia). Email: ragarcial@ufpso.edu.co; orcid: https//orcid.org/0000-0002-2734-1425

[2]Universidad Francisco de Paula Santander Ocaña (Colombia). Email: bargottai@ufpso.edu.co; orcid: https//orcid.org/0000-0003-1403-6533

[3]Universidad Francisco de Paula Santander Ocaña (Colombia). Email: wquinteroq@ufpso.edu.co; orcid: https//orcid.org/0000-0003-3260-6923

Received: 05-31-2020 Accepted: 10-28-2020

How to cite: García-León, Ricardo Andrés; Argotta-Hernandez, Breiner; Quintero-Quintero, Wilder (2020). Diseño de una máquina de termoconformados para la fabricación de filamento ABS Y PLA. *Informador Técnico*, *85*(1), 34-51. https://doi.org/10.23850/22565035.2865

Resumen

Durante el proceso de impresión 3D, alrededor del 15 % del material utilizado es desperdiciado, debido a los soportes y bases para generar los prototipos, atribuyendo un problema para el ambiente y la economía de los usuarios. Actualmente, no existe una máquina de bajo costo con la que se pueda reciclar el filamento de acrilonitrilo butadieno estireno (ABS) y ácido poliláctico o poliácido láctico (PLA) de las impresoras 3D, y así lograr disminuir los costos de operación de este tipo de máquinas que son de gran uso en sectores industriales para la fabricación de prototipos. Para el diseño de la máquina de termoconformados de material reciclado de ABS y PLA, se utilizaron teorías de diseño mecánico, transferencia de calor y análisis numérico para calcular y analizar los elementos más importantes. Teniendo en cuenta lo anterior, las industrias que utilizan este tipo de polímeros podrán reciclar y fabricar el material de impresión, optimizando, además, el proceso productivo, reduciendo los tiempos de entrega y los costos de impresión mediante el uso de esta máquina. Finalmente, se podrán incrementar las propiedades mecánicas y térmicas de nuevos materiales a través de la adición de otros similares.

Palabras clave: ABS; PLA; termoconformado; temperatura; reciclaje; plástico.

Abstract

During the 3D printing process, around 15 % of the material used is wasted, due to the supports and bases to generate the prototypes, attributing a problem to the environment and the economy of the users. Currently, there is no low-cost machine that can recycle acrylonitrile butadiene styrene (ABS) and polylactic acid or polyacid lactic acid (PLA) filament from 3D printers, thus reducing operating costs for this type of machines that are widely used in industrial sectors for the manufacture of prototypes. For the design of the ABS and PLA recycled material thermoforming machine, theories of mechanical design, heat transfer, and numerical analysis

were used to calculate and analyze the most important elements. Considering the above, the industries that use this type of polymers will be able to recycle and manufacture the printing material, also optimizing the production process, reducing delivery times and printing costs by using this machine. Finally, the mechanical and thermal properties of new materials can be increased through the addition of similar ones.

Keywords: ABS; PLA; thermoforming; temperature; recycling; plastic.

1. Introduction

Extrusion is the most used process in the industry for the processing of plastics, considering that around 60 % of the total polymers transformed in Colombia have gone through some extrusion process (García-León; Bohorquez-Niño; Barbosa-Paredes, 2019). Likewise, the development of extrusion machine prototypes has taken certain steps to optimize resources and processes (Cifuente, 2001; Gómez; Gutiérrez, 2007; Morales; Castillo, 2006; Muñoz, 2008; Paredes, 2017; Urrego; Escobar, 2008; Vargas, Santiago; Patiño, 2008). Extrusion has its first signs in 1797, when Joseph Bramah recorded the first extrusion process to make lead pipes, which consisted of the preheating of the metal that then passed through a die with a plunger by hand. Then, in 1894, Alexander Dick carried out the extrusion process for copper and bronze alloys (García-León *et al.,* 2019). In 1935 Paul Troster built the first thermoplastic extruder in Germany (Ortiz; Acuña, 2018). But until 2010, fused polymer filament manufacturing was used to obtain low-cost, rapid prototyping systems. Therefore, extrusion is the ideal process for the manufacture of 3D printing filament (Fajardo; Cobos, 2011; Woern; McCaslin; Pringle; Pearce, 2018; Poudel, 2015).

3D printing technology allows fast and economical production of devices without machining or tools, making use of computer-aided design (CAD) (Cruz; Boudaoud; Camargo; Pearce, 2020). The growth of this technology has accelerated due to an improvement in additive manufacturing technologies and production speeds; therefore, the amount of 3D printed polymers will continue to increase (Lanzotti *et al.,* 2019) and, consequently, will increase waste generated by printing, which will affect the environment and manufacturing costs. Most 3D printers are manufactured to work with acrylonitrile butadiene styrene (ABS) or polyacid or polylactic acid (PLA) filaments due to their mechanical and physical properties, which are manufactured mainly in two standard diameters: 1.75 and 3.0 mm, which can be transported and pushed by the nozzle to be easily extruded (Luna; Valadez, 2016).

On the other hand, ABS is a thermoplastic that presents an amorphous molecular structure with high resistance to chemical substances, abrasives, and impacts, being widely used in the automobile industry and in household appliances, although it is not an ecological material, it can be recycled and reprocess it, it is also easy to mold (Mirón; Ferrándiz; Juárez; Mengual, 2017; Salim; Termiti; Saad, 2019). PLA is a thermoplastic and biodegradable aliphatic polyester that is derived from renewable sources rich in starch, such as corn, tapioca, and sugar cane, being an environmentally friendly material (Montealegre; González, 2015; Salim *et al.,* 2019).

Currently, several works have focused their studies on the recycling of thermoplastics such as ABS and PLA; also, the addition of other types of elements or components to improve their mechanical, physical, and structural properties (Cisneros-López *et al.,* 2020; Cruz *et al.,* 2020). Rigoussen, Raquez, Dubois, Verge (2019) reinforced the mechanical properties of PLA and ABS using cardanol as a compatibilizer, making use of the extrusion process. The results show that the materials had good compatibility and managed to improve impact resistance by 172 %. Lanzotti *et al.* (2019) conducted experiments on virgin and recycled PLA to verify the difference in mechanical properties through three different recycling processes. For their part, Goutham, Veena, and Prasad (2018) characterized and optimized parameters, such as filling density and ABS construction material, mixed with recycled material. They performed bending and three-point bending tests to determine the mechanical properties of the sample obtained by 3D printing.

In this research work, the main mechanical design and heat transfer calculations are shown, to establish a prototype of a thermoforming machine for the recycling of low-cost ABS and PLA material, derived from waste generated during the 3D printing process, with which optimization of the waste produced by this material and of the financial resources of the companies that use this class of systems to generate prototypes will be achieved. In addition, design tests of experiments with mixtures may be carried out to optimize the mechanical and structural properties of these types of materials.

2. Materials and Methods

The design of this research is documentary because various physical phenomena are related to achieving a design based on customer requirements, using theoretical foundations and a quantitative research approach, in this way, data and values are applicable to the reality for a future construction of the thermoforming machine. In addition, the methodology of the mechanical design process was considered to establish the specifications and requirements of potential customers, and, in this way, achieve the suitability and reliability of the machine for plastic extrusion based on theories, simulations, and similar references (Ullman, 2003). Figure 1 shows the methodology applied in the numerical design analysis of the thermoforming machine.

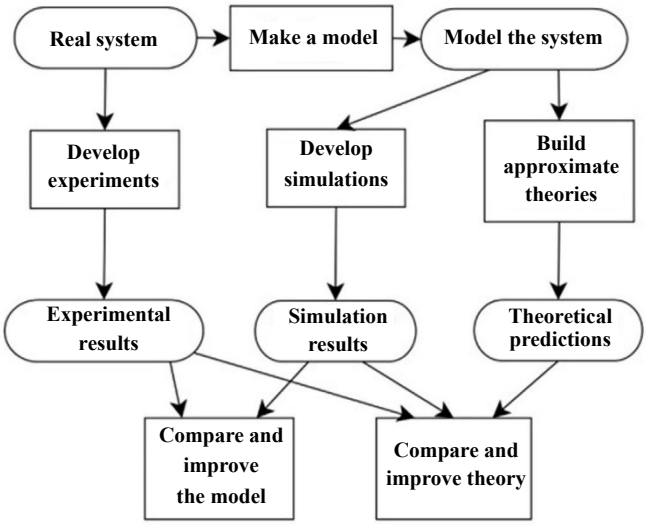

Figure 1. Applied methodology
Source: own elaboration.

The extrusion process begins when the pellets are fed into the chamber where the extruder screw rotates. Turning the screw causes the material to mix and advance through the hot chamber; the heat of the chamber together with the advancement of the screw causes the material to melt uniformly, to become a flow of malleable material that finally passes through the nozzle to acquire the desired cross-section. The extruded material requires a cooling process to solidify the part and obtain the desired profile at the end of the thermoforming process (Mena, 2018). SolidWorks Flow Simulation was used to perform the numerical analysis on the elements that support the greatest amount of stress, since it solves the Navier-Stokes equations, which are formulations of the laws of conservation of mass, momentum, and energy (Sobachkin; Dumnov; 2014; Thuresson, 2014).

Figure 2 shows the stages of the extrusion process:

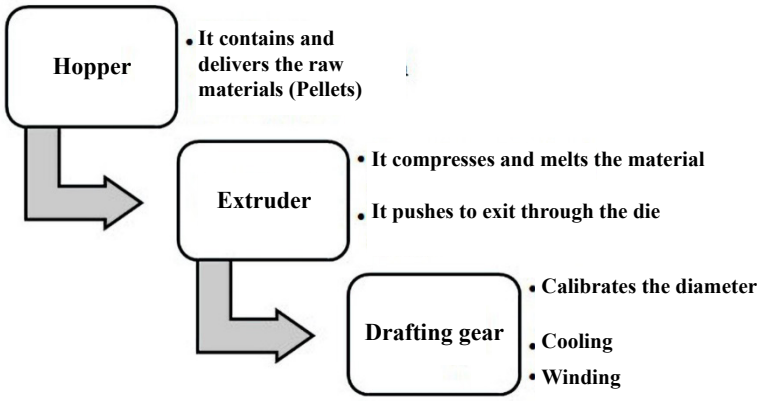

Figure 2. Stages of the extrusion process
Source: own elaboration.

The main components of an extruder for the manufacture of 3D printing filament are hopper, extruder screw, cylinder, heating system, die, and power system (Montealegre; González, 2015). For these calculations, machine design theories will be used considering the Shigley book (Budynas; Nisbett, 2017). On the other hand, for the calculation of the resistance, a thermal analysis is required, theories of heat transfer were used making use of the book (Cengel, 2007).

3. Analysis and discussion

To start the design process, the decision matrix of the two spindle models was carried out to select a winning design according to the market requirements, the needs, specifications of the clients and the researchers, for which a grading from 0 to 10 was applied as shown in Table 1.

Table 1.
Decision matrix

Criteria	Percentage of importance (%)	Extruder machine			
		Single-Screw		Twin-Screw	
		Rating	Weighting	Rating	Weighting
Less weight and size	50	8	4	4	2
Lower manufacturing cost	40	6	2.4	2	0.8
Ease of manufacture	20	8	1.6	7	1.4
Shorter manufacturing time	30	9	2.7	5	1.5
Better performance in composite materials	50	5	2.5	8	4
Ease of docking	20	6	1.2	4	0.8
TOTAL		-	14.4	-	10.5

Source: own elaboration.

Considering the above, Figure 3 shows the winning design of the thermoforming machine with each of the elements that comprise it.

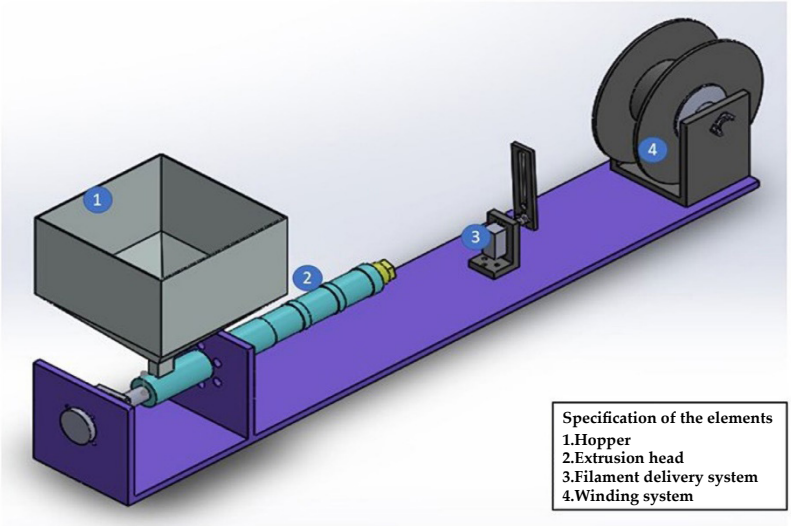

Figure 3. Winning conceptual design of the extrusion machine
Source: own elaboration.

3.1. Element Design

Considering the winning design, each of the elements that make up the machine was calculated as detailed below:

3.1.1. Hopper

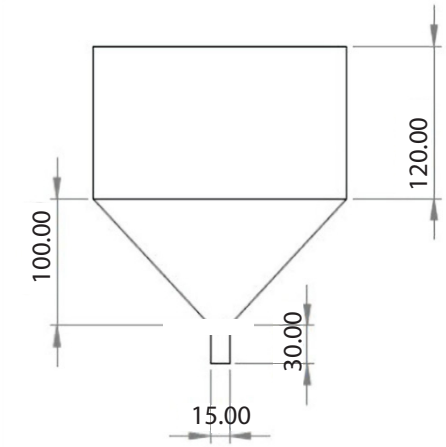

Figure 4. Hopper design
Source: own elaboration.

To maintain the dimensions of the machine, the hopper has a pyramidal shape with the following dimensions: height 25 cm, an upper area of 20 × 20 cm and a lower area of 1.5 × 2.5 cm as shown in Figure 4, which may support a total volume of 6286.19 cm^3. Additionally, the capacity of the hopper was determined with the weight of each ABS or PLA flake. The material of the hopper is AISI 304 grade stainless steel, with a thickness of 2.0 mm to guarantee resistance to heat and deformation during the thermoforming process.

On the other hand, the average volume of the flakes of 0.075 cm^3 was considered and, in this way, an approximate value of the weight of the flakes was obtained. Subsequently, it is assumed that a flake will measure 0.5 cm long, 0.75 cm wide and 0.2 mm thick, so the capacity of the hopper is 7.6 kg. As a recommendation for use, the hopper should not be filled more than 70 %, that is, the nominal capacity of the hopper is 5.3 kg (Paredes, 2017; Argotta-Hernandez, 2019).

3.1.2. Extrusion head

The extrusion head consists of the breaker plate, filters, and the die. The function of the breaker plate is to mix the material and break the spiral flow pattern generated by the screw. In this element, the filters are located at the end of the extruder screw, which traps the impurities that can affect the process, the filters are located so that the coarse mesh is closer to the breaking plate (Mena, 2018). The selection of the breaker plate was made taking into account the SFR tooling virtual catalog, for which, only the internal diameter of the head sleeve was required. Thus, the open area of the plate was determined to be 0.13 in^2 = 83.87 mm^2. For the selection of the mesh, the specification of the stainless steel meshes of the AmbicaGroup company were used, where the meshes of denomination 60×60, 80×80 and 120×120 were selected. In this regard, the extrusion die is an interchangeable element on the machine. In this case, a matrix was designed to extrude a 1.75 mm filament and another for 3 mm, in addition, the contraction index of the material must be reviewed, since this influences the profile final diameter to be extruded (Mexpolimeros, 2019).

3.1.3. Spindle

It is the fundamental part of the extrusion machine, on this depends the production, application of the extruder, speed of rotation and design of the extrusion head (Brito, 2017).

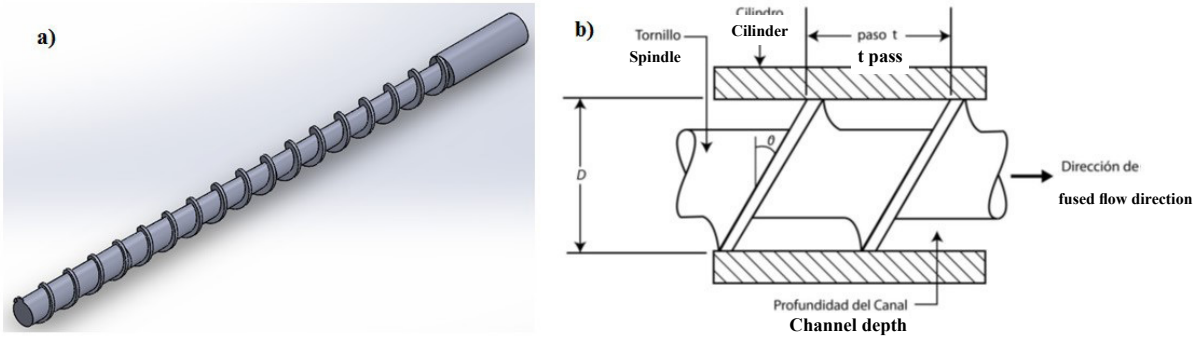

Figure 5. a) Geometric design of the spindle and b) Parts of the spindle
Source: own elaboration.

The choice of spindle parameters depends on the materials to be worked (ABS and/or PLA). In this way, a screw was selected for general use as shown in Figure 5a, that is, that allows working both materials without losing efficiency. For this, three zones are defined in the spindle (feeding, compression, and dosing), and there will be one (1) single channel, with constant pitch and variable depth for each zone.

The ratio of the length (L) and diameter (D) of the spindle is of great importance, because when the length of the spindle increases, the effect of heat on the material, the turning speed, and the production improves. A typical ratio (L/D) for extruding thermoplastic polymers ranges from 20:1 to 30:1. Long screws are widely used for the manufacture of films, fibers, among others. For the manufacture of continuous profiles, short spindles are recommended (Brito, 2017). For the extrusion of cables or filaments, a higher extrusion pressure is required,

then the degree of compression used must be low, also, a smaller depth in the helical channel in the dosing zone is recommended when manufacturing filaments. Considering the above, a compression degree of 2 is chosen, with this there is a small depth in the dosing area and a greater depth in the feeding area, thus obtaining a pressure gradient (Brito, 2017).

The parameters selected for the spindle are based on the final measurements of the machine and the aforementioned parameters are maintained according to Figure 5b. Therefore, the following parameters were established for the machine: total length of the spindle (Lt) = 400 mm; spindle length (L) = 340 mm; spindle stem length (le) = 60 mm; screw diameter (D) = 20 mm; L/D ratio = 17; number of fillets = 17 and degree of compression (i) = 2. Considering the design theories, the following additional calculations were carried out: spindle pitch (t) = 20 mm; fillet width (e) = 2 mm; channel depth in the feeding zone (h1) = 4 mm; channel depth in the dosing zone (h3) = 2 mm; the diameter of the web (d) = 12 mm; helix angle (φ) = 17.6 °; length of feed zone (La) = 140 mm; length of compression zone (Lc) = 120 mm and length of dosing zone (Ld) = 80 mm.

3.1.4. Nozzle

Figure 6 shows the internal geometry of the nozzle, which has a conical section that is responsible for reducing the diameter of the cylinder to the diameter to be obtained. For the exterior part, it is required to know the manufacturing material, so that the minimum wall thickness can be calculated. The nozzle will be made of 360 brass, because it is an easy-to-machine material with good thermal conductivity, with allowable stress of 310 MPa.

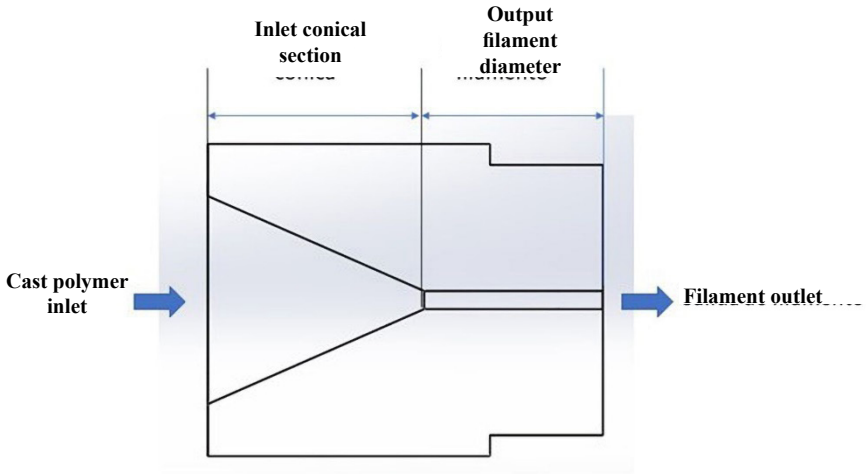

Figure 6. Geometry of the nozzle
Source: own elaboration.

Subsequently, a thickness of 5 mm was defined by design theories, which has a safety factor of 1.45, establishing the following design measures: inlet internal diameter = 20 mm, outlet internal diameter = 2 mm, outside diameter = 30 mm, length of the conical section 20 mm and the length of the outlet section = 15 mm.

Figure 7 shows the calculation of the production; therefore, various speeds were recorded to find the one that best fits the two materials and the different nozzles.

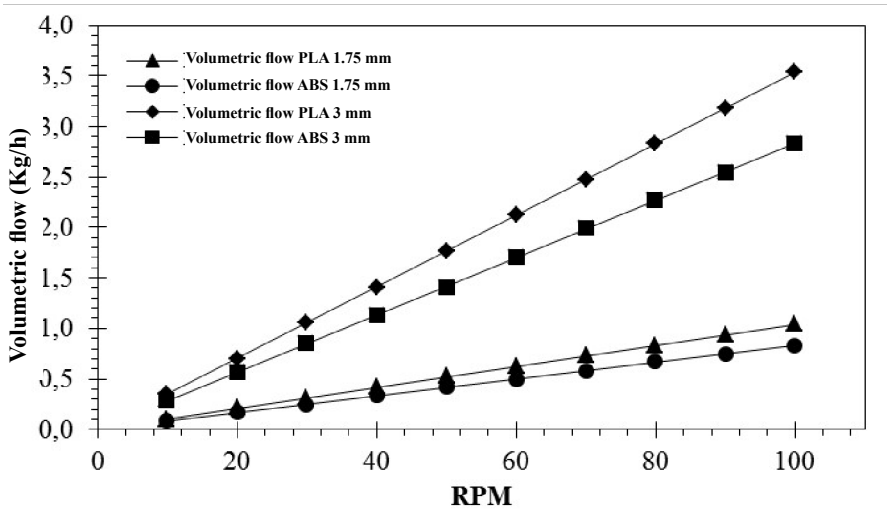

Figure 7. Nozzle flow growth slope
Source: own elaboration.

The effective viscosity is determined as a function of the shear rate by means of design diagrams for different materials as a function of the working temperature. The shear speed will depend on the geometric shape of the spindle channel (Paredes, 2017), for which a value of γ = 836 [1/s] was obtained. According to the cutting speed, it is necessary to obtain the effective viscosity of each material to be worked (ABS or PLA). In this way, the highest magnitude effective viscosity was used to obtain the maximum working pressure that can occur in the extruder. In the case of PLA, the working temperature will be 160 to 230 °C, so the effective viscosity will be evaluated at the average working temperature, approximately 190 °C. For ABS, the working temperature will be 215 to 250 °C, so the effective viscosity will be evaluated at the average working temperature, approximately 230 °C, according to (Altinkaynak; Gupta; Spalding; Crabtree, 2011), under the following conditions: shear speed equal to 836 [1/s] and effective viscosity of 400 MPa.

On the other hand, the maximum pressure in the screw is generated when there is no flow movement inside the cylinder, obtaining a value of 181.3 MPa. Also, the pressure at the nozzle is 106.43 MPa. The working power of the spindle must be necessary to rotate the spindle at the revolutions per minute (rpm) required for extrusion of the material, which depends on the power necessary to displace the material and the energy consumed by the cylinder clearance, according to the results obtained by (Brito, 2017), obtaining a value of 253.53 W = 0.34 HP. Based on the spindle sizing, a motor was selected that meets the criteria and provides a certain margin of safety. The selected motor was a high torque geared motor that works at 12 V Direct Current. (DC) and delivers a speed of 100 rpm. For this element, AISI 4140 steel was selected as a material, due to its chemical composition of chromium and molybdenum, which gives the material high hardness and resistance to corrosion at temperatures of more than 540 °C, without losing its mechanical properties.

3.1.5. Cylinder

For the design of the cylinder, the clearance between the helical fillet and the barrel, and the diameter of the screw, were considered. First, the calculation of the inside diameter of the desired cylinder was carried out. This cylinder must cover the useful area of the spindle, so it will have a minimum length of 340 mm as shown in Figure 8. The minimum thickness that the cylinder must have to withstand the pressures requires knowing the cylinder material, therefore, an AISI 1020 CD steel was selected, with allowable stress of 390 MPa. This material was chosen considering the following parameters: working temperatures, availability, manufacturing, wear resistance, corrosion, resistance and cost. The cylinder will have a final thickness of 10 mm and a thickness of 8.5 mm in the threaded part. This thickness depends on the type of thread, in this case, it is a fine thread that is

obtained in this way, by means of a safety factor with the following values: FScilin = 2.13 and FSpf = 1.81. For the manufacture of the spindle, a 42 mm diameter bar will be used for a length of 500 mm, which is roughly equivalent in commercial bars in the country to a diameter of 1-5/8".

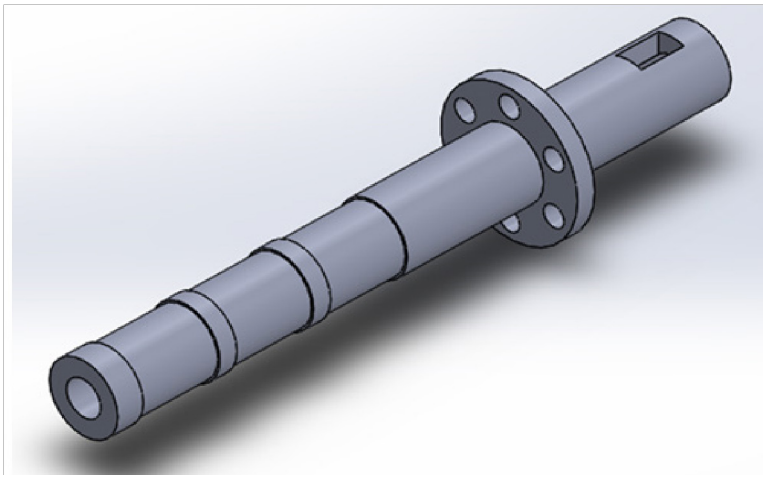

Figure 8. Conceptual design of the cylinder
Source: own elaboration.

3.1.6. Heating system

The power required for the electrical resistors was calculated considering that the power is a function of the necessary heat generated by the resistors, transferred to the cylinder and the spindle. For the design, it was taken that the heat flow is one-dimensional, with a stationary regime, as shown in Figure 9:

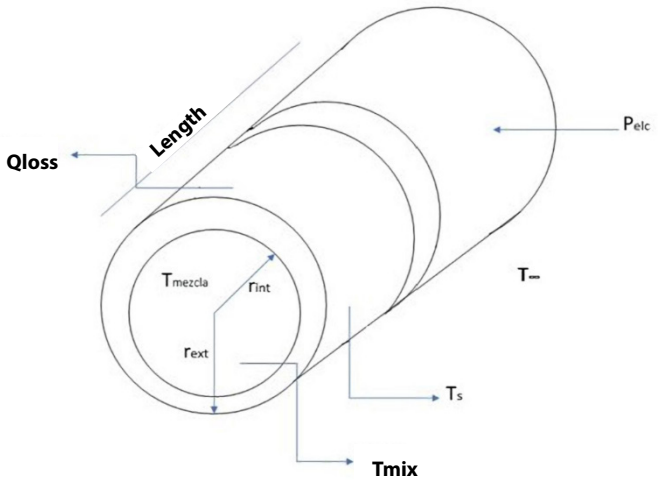

Figure 9. Cylinder model and heating system
Source: own elaboration.

Figure 10 shows the sketch of the heating system, in addition, the electrical analogy is clarified for the calculation of the power required to melt the (working) mixture, plus the losses that exist in the environment (conduction, convection, and radiation), which must be equal to the electrical power that the heater must deliver.

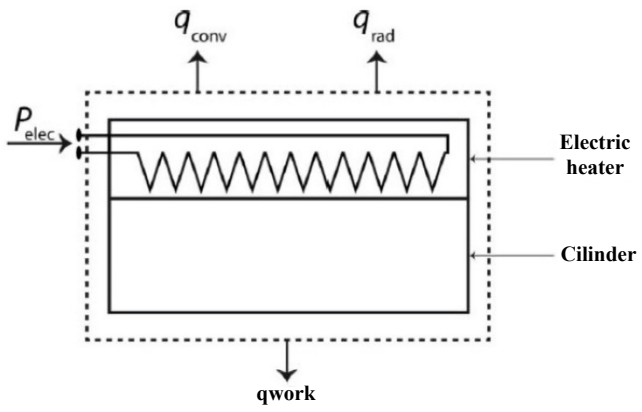

Figure 10. Sketch of the heating system
Source: own elaboration.

Defining the general equation for the required power we have as a result Equation 1:

$$q_{elec} = q_{trabajo} + (q_{conv} + q_{rad}) = q_{trabajo} + q_{perd} \quad (1)$$

Where: q_{elec} is the power delivered by the electric heater [W], q_{conv} is the power lost to the environment through convection [W], q_{rad} is the power lost to the environment through radiation [W], q_{work} is the power necessary to carry the mixture at the working temperature [W], and q_{loss} is the power lost to the environment [W]. When calculating the working power, it is necessary to know the operating temperatures, and as two materials are intended to be used, there are two different operating temperatures, for ABS it will be 230 °C and for PLA it will be 190 °C. For both, the ambient temperature is 22 °C. Since the polymers are amorphous (Brito, 2017), there is no latent heat of the fusion zone, so no additional energy is necessary for the phase change. Equation 2 is used to calculate the heat of work:

$$q_{trabajo} = \dot{m} * C_p * (T_m - T_i) \quad (2)$$

Where: $\dot{m}$ is the mass flow of material [kg/s], C_p is the specific heat of the material [J/kg °C], T_m is the temperature of the mixture [°C] and is the ambient temperature [°C], obtaining the results shown in Table 2:

Table 2.
Working heat result for different nozzles

Variable	Description	Value	Unit
qtABS - 1.75	ABS working heat with 1.75mm nozzle	87.84	W
qtPLA - 1.75	ABS working heat with 1.75mm nozzle	60.45	W
qtABS - 3	ABS working heat with 3 mm nozzle	298.99	W
qtPLA - 3	ABS working heat with 3 mm nozzle	205.84	W

Source: own elaboration.

To calculate the losses to the environment, it is necessary to calculate the thermal resistance of the system (Brito, 2017). Said resistance will depend on the heat exchange of the cylinder with the environment, through the phenomenon of convection and radiation. For this, Equations 3 and 4 are used.

$$R_{conv} = \frac{1}{h \times A_s} \quad (3)$$

$$R_{rad} = \frac{1}{A_s \times \varepsilon \times \sigma \times (T_s^2 + T_i^2) \times (T_s + T_i)} \quad (4)$$

Where: h is the heat transfer coefficient in natural convection [W/m^2 °C], A_s is the area of the surface exposed to convection [m^2], ε is the emissivity of the material (0.865 for AISI 1020 CD) [-], σ is the Stefan-Boltzmann constant =5.6710^{-8} [W/m2k4], T_s is the absolute temperature of the surface [K] and T_i is the absolute temperature of the environment [K].

Replacing in the equations, we have: Rconv= 2.43 - Rrad-ABS = 1.83 -Rrad-PLA = 2.1

Table 3 shows the calculations of heat losses by convection and radiation.

Table 3.
Calculation of radiation and convection losses

Variable	Description	Value	Unit
qPer - ABS - conv	Convection heat losses for ABS	81.48	W
qPer - PLA - conv	Convection heat losses for PLA	69.14	W
qPer - ABS - Rad	Radiation heat losses for ABS	1082	W
qPer - PLA - Rad	Radiation heat losses for PLA	80	W

Source: own elaboration.

The total power that the band must deliver is the working power plus the losses and the data is summarized in Table 4:

Table 4.
Total power required

Variable	Description	Value	Unit
qElc-ABS-D1.75	Total power for ABS with 1.75 [mm] nozzle	277.52	W
qElc-PLA-D1.7	Total power for PLA with 1.75 [mm] nozzle	209.59	W
qElc-ABS-D3	Total power for ABS with 3 [mm] nozzle	488.67	W
qElc-PLA-D3	Total power for PLA with 3 [mm] nozzle	354.98	W

Source: own elaboration.

According to the table above, the maximum power required is 488.67 W corresponding to the 3 mm nozzle when using ABS. This value will be the reference value for the selection of resistors. For this system, three heating resistances distributed in the cylinder will be used to maintain a uniform temperature, it should be noted that the resistances will be in the sections corresponding to the transition and dosage to avoid clogging in the feeding zone. The resistors will have different powers distributed as follows: a 500 W resistor will be located at the cylinder output, followed by a 250 W resistor and, finally, a 150 W resistor.

3.1.7. Ventilation system

This system will use a fan for forced convection cooling. Its function is to reduce the temperature of the filament at the outlet of the nozzle, with that it is possible to avoid the expansion of the filament, reducing variations in the final diameter and having a higher quality of the filament. At this stage it is desired to reach a temperature higher than the glass transition temperature of the material, since below it the polymer is rigid and brittle, and above it, it is soft and flexible, providing the necessary characteristic for the winding system the extruder is working properly. To calculate this system, a fan must be preselected, in this case, an 80 × 80 × 10 mm fan with an angular speed of 3000 rpm, using Equation 5.

$$T = T_{\infty} + (T_0 + T_{\infty})e^{-\frac{4hx}{\rho V_e D C_p}} \qquad (5)$$

Where: T_{∞} is the ambient temperature [22 °C], T_0 is the filament outlet temperature [°C], h is the convection coefficient [W/m^{2}K], ρ is the density of the material [kg/m^3] , V_e is the nozzle filament exit velocity [m/s], D is the filament diameter [m], C_p is the material specific heat [J/kg ° C], and x is the position to be evaluated. The results are summarized in Table 5:

Table 5.
Temperature at the nozzle outlet

Variable	Description	Value	Unit
$T_{D1.75\text{-}ABS}$	Temperature at 24 [cm] when exiting the nozzle 1.75 [mm] for ABS	131.1	°C
$T_{D3\text{-}ABS}$	Temperature at 24 [cm] when exiting the nozzle of 3 [mm] for ABS	179.2	°C
$T_{D1.75\text{-}PLA}$	Temperature at 24 [cm] when exiting the nozzle 1.75 [mm] for the ABS	126.2	°C
$T_{D3\text{-}PLA}$	Temperature at 24 [cm] when exiting the nozzle of 3 [mm] for the PLA	161.6	°C

Source: own elaboration.

From the results it is observed that the filament when passing through the fan reduces its temperature but keeps it above the glass transition temperature of the ABS and PLA (115 °C and 60 °C, respectively) in both nozzles, presenting better efficiency for the 1.75 mm nozzle. However, the filament in both cases will be more stable avoiding diameter variations and it will be possible to work in optimal conditions in the winding system of the extruder. From the calculations made previously, the system will have three fans in series. It was chosen: an 80×80×25 mm QG brand fan, which has a high performance delivering 47 CFM of flow at 3000 rpm and operating at 12 V direct current.

3.1.8. Filament spreader selection

To select the dealer, an average time of 377 s was taken for each pass. From this result, a feetech FS5115M servo motor was selected. It is a 6V high torque direct current motor with 180° rotation.

3.2. Numerical analysis of the main elements of the machine

3.2.1. Spindle

For the static analysis of the spindle, its weight was considered, with respect to the thermal analysis the spindle will be subjected to the heat that is transferred from the molten polymer in a transitory state, as shown in Table 6.

Table 6.
Spindle characteristics for numerical analysis

Name	Spindle for extrusion	Units
Material	AISI 4140	
Weight	0.59	Kg
Elastic Limit	4.7 X 10^{-8}	N/m^2
Traction limit	7.45X10^{8}	N/m^2
Elastic modulus	2.05X10^{11}	N/m^2
Coefficient of Poisson	0.285	-
Density	7850	Kg/m^3
Shear modulus	8X10^{10}	N/m^2
Coefficient of thermal dilation	1.23X10^{-5}	K
Mesh type	Solid mesh	-
Number of nodes	49032	-

Source

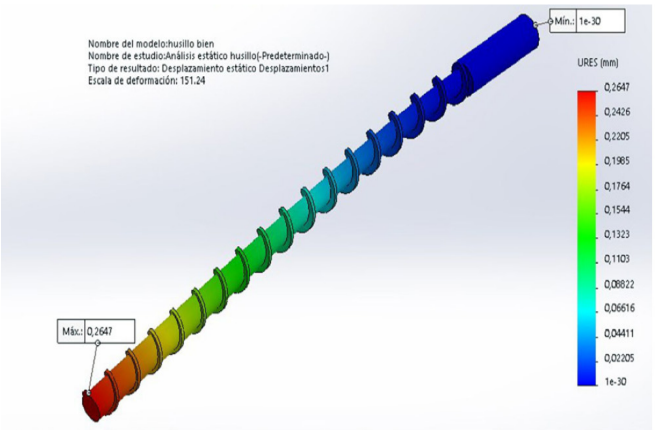

Spindle Static Analysis Results

Table 6 shows that the deformation is very low, with a value of 0.26 mm similar to different studies reported in the literature. This clearance will be reduced with the help of the bearings and the rotation of the spindle, adjusting to the existing gap between the spindle and the extrusion cylinder. In addition, the molten polymer will act as a barrier between both elements (Flórez; García-León; Escobar, 2017; García-León; SuárezCastrillón, 2016).

Figure 11 shows the thermal analysis in the spindle, considering the factor of multiplication of the power of the resistances, due to the influence of the pressure and friction of the plastic with the walls and the blades of the spindle; where the temperature is close enough to the desired temperature at the tip of the spindle, which corresponds to 10 degrees Celsius below the temperature determined in the design conditions.

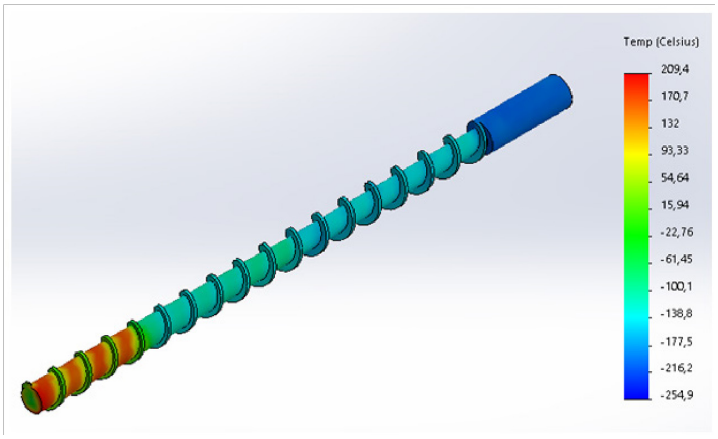

Figure 11. Results of the thermal analysis of the spindle
Source: own elaboration.

3.2.2. Cylinder

For the static analysis of the cylinder, it was subjected only to the pressure that is exerted from the temperature differences and the compression of the fluid in a transitory state. Cylinder characteristics are shown in Table 7:

Table 7.
Extrusion cylinder features

Name	Spindle for extrusion	Units
Material	AISI 1020 CD	-
Default error criterion	Von stress Mises max	-
Elastic limit	$3.51x10^8$	N/m^2
Traction limit	$4.21x10^8$	N/m^2
Elastic modulus	$2x10^{11}$	N/m^2
Coefficient of Poisson	0.29	-
Density	7900	Kg/m^3
Shear modulus	$7.7x10^{10}$	N/m^2
Coefficient of thermal dilation	$1.77x10^5$	xxxK
Mesh type	Solid mesh	-
Number of nodes	30535	-

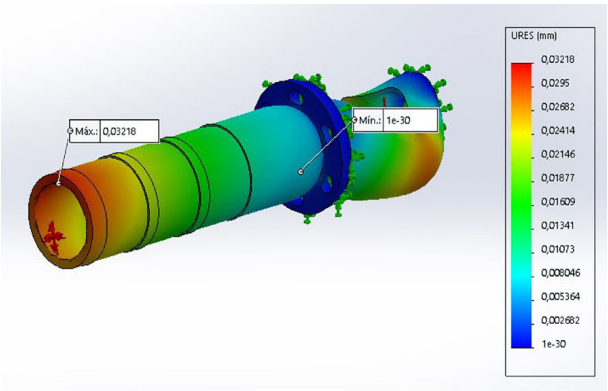

Spindle Static Analysis Results

Source: own elaboration.

Table 7 shows that the deformation is very low, with a value of 0.003 mm like different studies reported in the literature. The numerical analysis confirmed that the maximum pressure "s" occurs at the tip of the cylinder (Flórez *et al.*, 2017). Due to in that section is where the polymer is compressed and the average temperature of that last section is higher than the others, the deformation that may occur is very small, therefore, it is concluded that the material and the selected thickness for the cylinder it was adequate, complying with the design specifications (Flórez-Solano; García-León; Sánchez-Ortiz, 2017).

Figure 12 shows the thermal analysis of the cylinder. In this thermal analysis it is possible to observe the heat that is transferred to the cylinder from the heating resistances directly and the heat that is transferred from the air, a heat flow was applied by convection with an ambient temperature of 22 °C; as it is a transitory state, it was established as the initial temperature (García-León; Pérez, 2017).

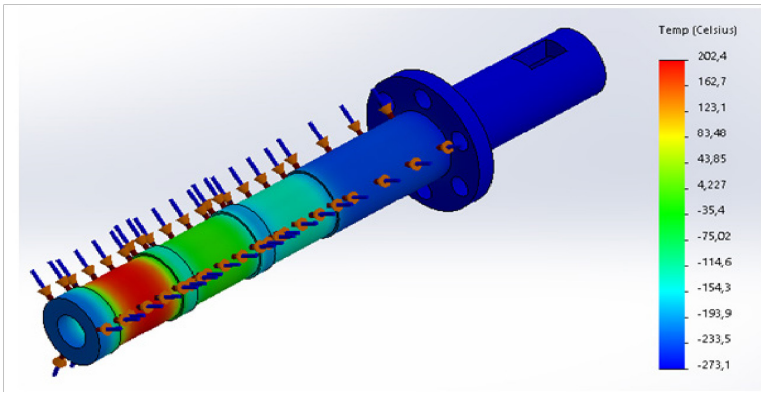

Figure 12. Results of cylinder thermal analysis
Source: own elaboration.

At the tip of the cylinder, the highest temperature is evidenced with an approximate value of 202 °C, obtaining a positive response on the heat transfer behavior for the selected design (García-León; Flórez-Solano; Pérez-Rojas, 2015).

3.2.3. Hopper

A static analysis was carried out on the hopper to corroborate the efforts that can be generated, in this case, those caused by the weight of the plastic pellets, considering the characteristics of Table 8:

Table 8.
Feed hopper features

Name	Spindle for extrusion	Units
Material	AISI 304 CD	-
Default error criterion	Von stress Mises max	-
Elastic limit	$2.07x10^8$	N/m^2
Traction limit	$5.17x10^8$	N/m^2
Elastic modulus	1.9x1011	N/m^2
Coefficient of Poisson	0.29	-
Density	7900	Kg/m^3
Shear modulus	7.7x1010	N/m^2
Coefficient of thermal dilation	$1.8x10^{-5}$	Kelvin
Mesh type	Solid mesh	-
Number of nodes	30535	-

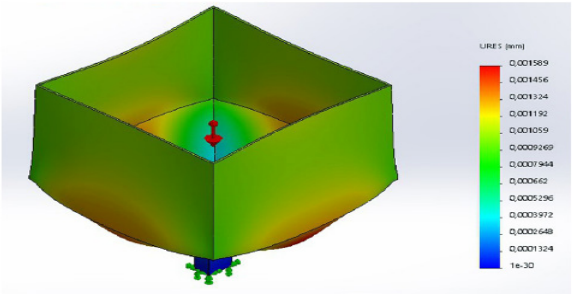

Hopper Static Analysis Results

Source: own elaboration.

The static analysis of the hopper showed that the material chosen for its manufacture correctly meets the design specifications, since, in stresses, its elastic limit is above the efforts calculated by the software and in deformations, with a minimum value of 0.00012 mm, as shown in Table 8.

4. Conclusions

A design was made that proposed two types of material to be extruded (ABS and PLA), in addition to allowing the coupling of different nozzles, in this case, one of 1.75 mm and one of 3 mm, dimensions corresponding to the diameters of the most commercial filament in the 3D printing industry. In the design of the elements that make up the extruder, it was ensured that the safety factor was greater than or equal to 1.2, to guarantee an optimal design.

For the installation of the extrusion head, the order of 60/80/120 must be considered, for the change verification a pressure limit of 25 % higher than the normal working pressure must be considered, when this occurs, the filter must be disassembled and cleaned, or if it needs to be changed.

With SolidWorks software, each part of the machine was modeled, and, in turn, its assembly was carried out. The assembly allowed to ensure a correct design and the precise and necessary measurements for its subsequent construction. In addition, the finite element analysis was implemented, applying static and thermal analysis to the elements with the greatest stress in the machine. These elements were the spindle, the cylinder, and the hopper, and, in this way, a correct design of the selected elements and materials was corroborated.

5. References

Altinkaynak, A.; Gupta, M.; Spalding, M.; Crabtree, S. (2011). Melting in a single screw extruder: Experiments and 3D finite element simulations. *International Polymer Processing*, 26(2), 182–196. https://doi.org/10.3139/217.2419

Argotta-Hernandez, Breiner (2019). *Diseño de una máquina de materiales termoconformados para la fabricación de filamento ABS y PLA para impresoras 3D* (tesis de pregrado). Universidad Francisco de Paula Santander Ocaña, Colombia.

Brito, Nicolás (2017). *Diseño de extrusora de filamento para impresión 3D a partir de plásticos reciclados* (tesis de pregrado). Universidad Técnica Federico Santa María, Chile.

Budynas; Richard; Nisbett, Keith (2017). *Mechanical Engineering Design de Shigley* (9a Edition). EE.UU.: McGraw-Hill.

Cengel, Yunus (2007). *Transferencia de calor y masa* (3ª Edición). México: McGraw-Hill.

Cifuente, Roosevelth (2011). *Diseño de una máquina extrusora para la empresa Plastik de Occidente* (tesis de pregrado). Universidad del Valle, Cali, Colombia.

Cisneros-López, Erick; Pal, Akhilesh; Rodriguez, Arturo; Wu, Feng; Misra, Manju; Mielewski, Deborah; Kiziltas, Alper; Mohanty, Amar (2020). Recycled poly (lactic acid)–based 3D printed sustainable biocomposites: a comparative study with injection molding. *Materials Today Sustainability*, 7–8, 100027. https://doi.org/https://doi.org/10.1016/j.mtsust.2019.100027

Cruz, Fabio; Boudaoud, Hakim; Camargo, Mauricio; Pearce, Joshua (2020). Plastic recycling in additive manufacturing: A systematic literature review and opportunities for the circular economy. *Journal of Cleaner Production*, 264, 121602. https://doi.org/https://doi.org/10.1016/j.jclepro.2020.121602

Miròn, V.; Ferràndiz, Santiago; Juàrez, David; Mengual, Ana. (2017). Manufacturing and characterization of 3D printer filament using tailoring materials. *Procedia Manufacturing*, 13, 888–894. https://doi.org/10.1016/j.promfg.2017.09.151

Flórez-Solano, Eder; García-León, Ricardo; Sánchez-Ortiz, Edgar (2017). Diseño de un sistema alimentador para un horno rotatorio en la producción de fosfato en Norte de Santander. *Revista Colombiana de Tecnologías de Avanzada*, 1(29), 70–80. https://doi.org/10.24054/16927257.v29.n29.2017.2489

Flórez, Eder; García-León, Ricardo; Escobar, Marlon (2017). Modelo de equipo de prensado tipo palanca, para mejorar la producción de queso en la provincia de Ocaña. *Revista Colombiana de Tecnologías de Avanzada*, 2(28), 140–149. https://doi.org/10.24054/16927257.v28.n28.2016.2477

García-León, Ricardo; Bohórquez-Niño, A.; Barbosa-Paredes, J. (2019). Design of an extrusion machine for the manufacture of plastic tubes. *Journal of Physics: Conference Series*, 1257, 12006. https://doi.org/10.1088/1742-6596/1257/1/012006

García-León, Ricardo; Flórez-Solano, Eder; Pérez-Rojas, Eduar (2015). Diseño de una máquina amasadora y laminadora automática de masa para pan. *Revista Ingenio UFPSO*, 8(1), 59–71.

García-León, Ricardo; Pérez, Eduar (2017). Analysis of the amount of heat flow between cooling channels in three vented brake discs. *Ingeniería y Universidad*, 21(1), 71–96. https://doi.org/10.11144/Javeriana.iyu21-1.aahf

García-León, Ricardo; Suárez-Castrillón, Sir (2016). Diseño de un prototipo de sembradora mecánica de granos, alternativa agrícola. *Ingenio UFPSO*, 12(2011–642X), 33–40.

Gómez, Jimmy; Gutiérrez, Jorge (2007). *Diseño de una extrusora para plásticos* (tesis de pregrado). Universidad Tecnológica de Pereira, Risaralda, Colombia.

Goutham, R.; Veena, T.; Prasad, K. (2018). Study on mechanical properties of recycled Acrylonitrile Butadiene Styrene (ABS) blended with virgin Acrylonitrile Butadiene Styrene (ABS) using Taguchi method. *Materials Today: Proceedings*, 5(11), 24836–24845. https://doi.org/10.1016/j.matpr.2018.10.282

Lanzotti, Antonio; Martorelli, Massimo; Maietta, Saverio; Gerbino, Salvatore; Penta, Francesco; Gloria, Antonio (2019). A comparison between mechanical properties of specimens 3D printed with virgin and recycled PLA. *Procedia CIRP*, 79, 143–146. https://doi.org/10.1016/j.procir.2019.02.030

Luna, Manuel; Valadez, Brenda (2016). Elaboración de filamentos de PLA, In: Memorias del Congreso Internacional de Investigación Academia Journals en Tecnologías Estratégicas Colima (pp. 17–21). Villa de Álvarez, Colima, México.

Fajardo, Jorge; Cobos, Cristian (2011). *Diseño de un sistema de extrusión-peletizado para el procesamiento de residuos plásticos para la empresa municipal de la ciudad de Cuenca EMAC*. Recuperado de: https://dspace. ups.edu.ec/bitstream/123456789/11164/1/Diseno%20de%20un%20sistema%20de%20extrusion%20 peletizado%20para%20el%20procesamiento%20de%20los%20residuos%20plasticos%20para%20la%20 Empresa%20Municipal%20de%20Aseo%20de%20Cuenca%20EMAC.pdf

Mena, Adrián (2018). *Diseño de una máquina extrusora de filamento termoplástico alimentada por desechos plásticos* (tesis de pregrado). Universidad de Costa Rica, Costa Rica.

Montealegre, Cristóbal; González, Luis (2015). *Diseño de una extrusora para filamento de impresión 3D* (tesis de pregrado). Universidad de Chile, Santiago de Chile.

Morales, Paola; Castillo, Jimmy (2006). *Metodología para el diseño de tornillos de máquinas extrusoras monohusillo*. Colombia: Universidad Autónoma de Colombia.

Muñoz, J. (2008). *Diseño y automatización de máquina extrusora para reciclaje plástico* (tesis de pregrado). Universidad Autónoma de Occidente, Santiago de Cali, Colombia.

Ortiz, Cristian, Acuña, Fausto (2018). *Departamento de Ciencias de la Energía y Mecánica* (tesis de pregrado). Universidad de las Fuerzas Armadas ESPE. Ecuador.

Paredes, Jhon (2017). *Diseño de una máquina extrusora de plástico para los productores de manguera de Ocaña*. (tesis de pregrado). Universidad Francisco de Paula Santander, Ocaña, Colombia.

Poudel, Bijaya (2015). *How to make Portable Homemade Filament Extruder* (tesis de pregrado). Arcada.

Rigoussen, Alan; Raquez, Jean-Marie; Dubois, Philippe; Verge, Pierre (2019). A dual approach to compatibilize PLA/ABS immiscible blends with epoxidized cardanol derivatives. *European Polymer Journal*, 114, 118–126. https://doi.org/https://doi.org/10.1016/j.eurpolymj.2019.02.017

Mexpolimeros (2019). *Producción, importación, distribución y comercialización de polímeros termoplásticos y elastómeros.* Recuperado de: https://www.mexpolimeros.com/contracci%C3%B3n.html

Salim, Mohd; Termiti, Zarif; Saad, Adzni (2019). Mechanical Properties on ABS/PLA Materials for Geospatial Imaging Printed Product using 3D Printer Technology. *Reference Module in Materials Science and Materials Engineering*. https://doi.org/https://doi.org/10.1016/B978-0-12-803581-8.11357-8

Sobachkin, A.; Dumnov, G. (2014). *Base numérica de CFD integrada en CAD. Informe Técnico.* https://www. solidworks.es/sw/docs/Flow_Basis_of_CAD_Embedded_CFD_Whitepaper_ESP.pdf

Thuresson, Adrian (2014). CFD and Design Analysis of Brake Disc (tesis de maestría). University of Technology, Gothenburg, Sweden.

Ullman, D. (2003). *The Mechanical Design Process*. México: McGraw Hill.

Urrego, Juan; Escobar, Luis (2008). *Modelación paramétrica y manufactura de mezcladores para extrusión de termoplásticos utilizando sistemas CAD-CAM* (tesis de pregrado). Universidad EAFIT, Medellín, Colombia.

Vargas, Rubiel; Santiago, Roció; Patiño, M. (2008). Diseño y Construcción de un Controlador de Temperatura Programable para una Máquina Extrusora. *Revista Colombiana de Física*, 40(2), 385-387.

Woern, Aubrey; McCaslin, Joseph; Pringle, Adam; Pearce, Joshua (2018). RepRapable Recyclebot: Open source 3-D printable extruder for converting plastic to 3-D printing filament. *HardwareX*, 4, e00026. https://doi.org/10.1016/j.ohx.2018.e00026